



Heriot-Watt University
Research Gateway

Ultra-high photoluminescent quantum yield of β -NaYF₄: 10% Er³⁺ via broadband excitation of upconversion for photovoltaic devices

Citation for published version:

Maddougall, SKW, Ivaturi, A, Marques-hueso, J, Krämer, KW & Richards, BS 2012, 'Ultra-high photoluminescent quantum yield of β -NaYF₄: 10% Er³⁺ via broadband excitation of upconversion for photovoltaic devices', *Optics Express*, vol. 20, no. S6, pp. A879-A887.
<https://doi.org/10.1364/OE.20.00A879>

Digital Object Identifier (DOI):

[10.1364/OE.20.00A879](https://doi.org/10.1364/OE.20.00A879)

Link:

[Link to publication record in Heriot-Watt Research Portal](#)

Document Version:

Publisher's PDF, also known as Version of record

Published In:

Optics Express

General rights

Copyright for the publications made accessible via Heriot-Watt Research Portal is retained by the author(s) and / or other copyright owners and it is a condition of accessing these publications that users recognise and abide by the legal requirements associated with these rights.

Take down policy

Heriot-Watt University has made every reasonable effort to ensure that the content in Heriot-Watt Research Portal complies with UK legislation. If you believe that the public display of this file breaches copyright please contact open.access@hw.ac.uk providing details, and we will remove access to the work immediately and investigate your claim.

Ultra-high photoluminescent quantum yield of β -NaYF₄: 10% Er³⁺ via broadband excitation of upconversion for photovoltaic devices

Sean K. W. MacDougall,¹ Aruna Ivaturi,¹ Jose Marques-Hueso,¹ Karl W. Krämer,²
and Bryce S. Richards^{1,*}

¹*Institute of Photonics and Quantum Sciences, Heriot-Watt University, Edinburgh, EH14 4AS, Scotland*

²*Department of Chemistry and Biochemistry, University of Bern, Freiestrasse 3, CH-3012 Bern, Switzerland*

**B.S.Richards@hw.ac.uk*

Abstract: The upconversion photoluminescent quantum yield (PLQY) of erbium-doped hexagonal sodium yttrium fluoride (β -NaYF₄: 10% Er³⁺) was measured under broadband excitation with full width half maxima ranging from 12 to 80 nm. A novel method was developed to increase the bandwidth of excitation, while remaining independent of power via normalization to the air mass 1.5 direct solar spectrum. The measurements reveal that by broadening the excitation spectrum a higher PLQY can be achieved at lower solar concentrations. The highest PLQY of $16.2 \pm 0.5\%$ was achieved at $2270 \pm 100 \text{ mW mm}^{-2}$ and is the highest ever measured.

© 2012 Optical Society of America

OCIS codes: (190.7220) Upconversion; (160.5690) Rare-earth-doped materials; (040.5350) Photovoltaic; (250.5230) Photoluminescence; (300.6420) Spectroscopy, nonlinear.

References and links

1. F. Wang, Y. Han, C. S. Lim, Y. Lu, J. Wang, J. Xu, H. Chen, C. Zhang, M. Hong, and X. Liu, "Simultaneous phase and size control of upconversion nanocrystals through lanthanide doping," *Nature* **463**(7284), 1061–1065 (2010).
2. Z. Li, Y. Zhang, and S. Jiang, "Multicolor core/shell-structured upconversion fluorescent nanoparticles," *Adv. Mater.* **20**(24), 4765–4769 (2008).
3. P. Gibart, F. Auzel, J.-C. Guillaume, and K. Zahraman, "Below band-gap IR response of substrate-free GaAs solar cells using two-photon up-conversion," *Jpn. J. Appl. Phys.* **35**(8), 4401–4402 (1996).
4. A. Shalav, B. S. Richards, T. Trupke, K. W. Krämer, and H. U. Güdel, "Application of NaYF₄:Er³⁺ up-converting phosphors for enhanced near-infrared silicon solar cell response," *Appl. Phys. Lett.* **86**(1), 013505 (2005).
5. J. de Wild, J. K. Rath, A. Meijerink, W. G. J. H. M. van Sark, and R. E. I. Schropp, "Enhanced near-infrared response of a-Si:H solar cells with β -NaYF₄:Yb³⁺ (18%), Er³⁺ (2%) upconversion phosphors," *Sol. Energy Mater. Sol. Cells* **94**(12), 2395–2398 (2010).
6. W. Shockley and H. J. Queisser, "Detailed balance limit of efficiency of p-n junction solar cells," *J. Appl. Phys.* **32**(3), 510–519 (1961).
7. A. Shalav, B. S. Richards, and M. A. Green, "Luminescent layers for enhanced silicon solar cell performance: up-conversion," *Sol. Energy Mater. Sol. Cells* **91**(9), 829–842 (2007).
8. B. S. Richards and A. Shalav, "Enhancing the near-infrared spectral response of silicon optoelectronic devices via up-conversion," *IEEE Trans. Electron. Dev.* **54**(10), 2679–2684 (2007).
9. S. Fischer, J. C. Goldschmidt, P. Löper, G. H. Bauer, R. Bruggemann, K. Krämer, D. Biner, M. Hermle, and S. W. Glunz, "Enhancement of silicon solar cell efficiency by upconversion: optical and electrical characterization," *J. Appl. Phys.* **108**(4), 044912 (2010).
10. F. Auzel, "Upconversion and anti-stokes processes with f and d ions in solids," *Chem. Rev.* **104**(1), 139–174 (2004).
11. S. Ivanova and F. Pellé, "Strong 1.53 μm to NIR-VIS-UV upconversion in Er-doped fluoride glass for high-efficiency solar cells," *J. Opt. Soc. Am. B* **26**(10), 1930–1938 (2009).
12. S. Balushev, T. Miteva, V. Yakutkin, G. Nelles, A. Yasuda, and G. Wegner, "Up-conversion fluorescence: noncoherent excitation by sunlight," *Phys. Rev. Lett.* **97**(14), 143903 (2006).
13. S. Balushev, V. Yakutkin, T. Miteva, G. Wegner, T. Roberts, G. Nelles, A. Yasuda, S. Chernov, S. Aleshchenkov, and A. Cheprakov, "A general approach for non-coherently excited annihilation up-conversion: transforming the solar-spectrum," *New J. Phys.* **10**(1), 013007 (2008).

14. J. C. Goldschmidt, S. Fischer, P. Löper, K. W. Krämer, D. Biner, M. Hermle, and S. W. Glunz, "Experimental analysis of upconversion with both coherent monochromatic irradiation and broad spectrum illumination," *Sol. Energy Mater. Sol. Cells* **95**(7), 1960–1963 (2011).
15. K. W. Krämer, D. Biner, G. Frei, H. U. Güdel, M. P. Hehlen, and S. R. Lüthi, "Hexagonal sodium yttrium fluoride based green and blue emitting upconversion phosphors," *Chem. Mater.* **16**(7), 1244–1251 (2004).
16. J. Ballato, S. H. Foulger, and J. D. W. Smith, Jr., "Optical properties of perfluorocyclobutyl polymers. II. Theoretical and experimental attenuation," *J. Opt. Soc. Am. B* **21**(5), 958–967 (2004).
17. J. F. Suyver, A. Aebischer, D. Biner, P. Gerner, J. Grimm, S. Heer, K. W. Krämer, C. Reinhard, and H. U. Güdel, "Novel materials doped with trivalent lanthanides and transition metal ions showing near-infrared to visible photon upconversion," *Opt. Mater.* **27**(6), 1111–1130 (2005).
18. Y. Y. Cheng, T. Khoury, R. G. C. R. Clady, M. J. Y. Tayebjee, N. J. Ekins-Daukes, M. J. Crossley, and T. W. Schmidt, "On the efficiency limit of triplet-triplet annihilation for photochemical upconversion," *Phys. Chem. Chem. Phys.* **12**(1), 66–71 (2009).
19. M. A. Green, ed., "*Solar Cells: Operating Principles: Technology and System Applications*," (The University of New South Wales, Kensington, NSW 2033, 1982).
20. A. C. Pan, C. del Cañizo, E. Cánovas, N. M. Santos, J. P. Leitão, and A. Luque, "Enhancement of up-conversion efficiency by combining rare earth-doped phosphors with PbS quantum dots," *Sol. Energy Mater. Sol. Cells* **94**(11), 1923–1926 (2010).
21. J. C. Goldschmidt, P. Löper, S. Fischer, S. Janz, M. Peters, S. W. Glunz, G. Willeke, E. Lifshitz, K. Krämer, and D. Biner, "Advanced upconverter systems with spectral and geometric concentration for high upconversion efficiencies," *Proc. of IEEE Conference on Optoelectronic and Microelectronic Materials and Devices* (IEEE, 2008), pp. 307–311.
22. M. A. Schreuder, J. D. Gosnell, N. J. Smith, M. R. Warnement, S. M. Weiss, and S. J. Rosenthal, "Encapsulated white-light CdSe nanocrystals as nanophosphors for solid-state lighting," *J. Mater. Chem.* **18**(9), 970–975 (2008).
23. C. M. Johnson, P. J. Reece, and G. J. Conibeer, "Slow-light-enhanced upconversion for photovoltaic applications in one-dimensional photonic crystals," *Opt. Lett.* **36**(20), 3990–3992 (2011).
24. E. Verhagen, L. Kuipers, and A. Polman, "Field enhancement in metallic subwavelength aperture arrays probed by erbium upconversion luminescence," *Opt. Express* **17**(17), 14586–14598 (2009).

1. Introduction

Upconversion (UC) is a process whereby two or more low energy photons are converted into one high energy photon. This form of spectral conversion has generated significant interest in different fields, from 3D displays [1] to biological imaging [2]. Moreover, in the area of photovoltaics (PV) [3–5], it has been considered as a solution to reducing the intrinsic loss associated with the transmission of sub-bandgap photons, a major contribution to the Shockley-Queisser limit for a single junction solar cell [6]. An UC layer placed behind a PV device (UC-PV) can absorb the transmitted photons and convert them to wavelengths above the band edge of the semiconductor, thus generating useful charge carriers.

For the case of silicon (Si), which is the most widely used semiconductor for solar cells, the UC material of choice to date has been trivalent erbium (Er^{3+}) doped hexagonal sodium yttrium fluoride ($\beta\text{-NaYF}_4$) [7–9]. In this system, the embedded Er^{3+} ions absorb light in the 1460 – 1580 nm range ($^4\text{I}_{15/2} \rightarrow ^4\text{I}_{13/2}$, energy level transition) and emit at 980 nm ($^4\text{I}_{11/2} \rightarrow ^4\text{I}_{15/2}$) with high efficiency due to the low phonon energy of the fluoride host, which greatly limits non-radiative recombination. UC can be achieved via several mechanisms including sequential ground state absorption (GSA) and excited state absorption (ESA). However, the most efficient and dominant mechanism for Er^{3+} doped $\beta\text{-NaYF}_4$ is energy transfer upconversion (ETU). GSA/ESA occur when a single Er^{3+} ion is excited to an intermediate excited state from the ground level (Fig. 1, ①GSA, $^4\text{I}_{15/2} \rightarrow ^4\text{I}_{13/2}$) and a second photon is absorbed within the lifetime (typically within the order of a millisecond for Er^{3+}) of that level (①ESA, $^4\text{I}_{13/2} \rightarrow ^4\text{I}_{9/2}$). Multi-phonon relaxation from the upper excited state ($^4\text{I}_{9/2} \rightarrow ^4\text{I}_{11/2}$) leads to emission of an UC photon (dot/dash arrows). ETU requires two ions to be excited into the intermediate energy state, usually through GSA (black solid arrows, ②GSA). When one ion relaxes into the ground state (dotted black arrow ①ETU on the left), rather than the emission of a photon, the energy is transferred to the neighboring ion raising it into a higher excited state (steps ①, ② and ③ETU on the right, dotted arrows). This process is dependent on the

concentration of ions and at high powers can lead to saturation effects through energy migration and cross relaxation (see Auzel [10] for a detailed review).

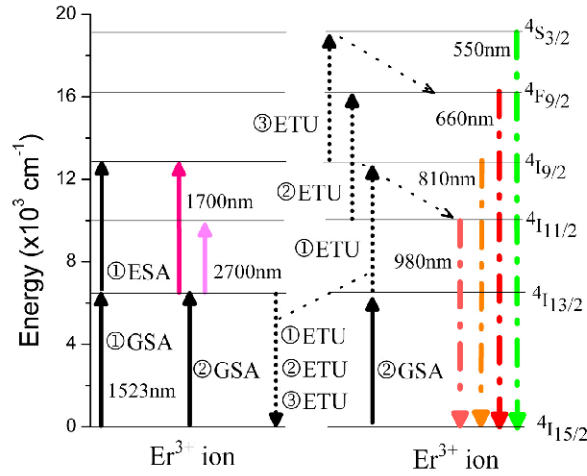


Fig. 1. Energy level diagram for two Er^{3+} ions in close proximity, which shows the various transitions possible to achieve UC emission. The peak wavelengths associated with UC mechanisms GSA/ESA (solid arrows), ETU (dotted arrows) and UC emission (dot/dash arrows) are shown.

Er^{3+} has an energy ladder with almost equidistant spacing, therefore infrared (IR) excitation at around 1523 nm can be used to achieve near infrared (NIR), visible and even ultraviolet (UV) emission through these UC mechanisms. Due to a strong resonance of 980 nm emission from 1523 nm monochromatic excitation, this has led to highest UC efficiencies being reported in the literature. Both Shalav *et al.* [7] and Fischer *et al.* [9] have reported the highest external quantum efficiencies (EQE) under 1523 nm monochromatic excitation for an UC-PV device using Er^{3+} doped $\beta\text{-NaYF}_4$. However, because of energy level broadening of each interacting level, UC is possible with bandwidths of around 100 nm. Although absorption at these wavelengths is lower and resonance weaker (under monochromatic excitation), they can still generate UC photons that can be effectively utilized by the overlying PV device. This opens up the opportunity to realize UC emission via broadband excitation centred around 1523 nm, as well as the possibility of contributions from both 1700 nm and 2700 nm excitation to populate the $^4\text{I}_{9/2}$ and $^4\text{I}_{11/2}$ levels, respectively, from the $^4\text{I}_{13/2}$ level (labelled solid arrows in Fig. 1). Therefore, an important research question for UC for PV applications is what enhancement of the UC process can be achieved under broadband excitation, rather than traditional monochromatic illumination.

UC in Er^{3+} has been shown to be most efficient at 1523 nm excitation [4, 7–9]. As the process is non-linear with respect to power, the majority of research has predominantly used high power monochromatic sources such as lasers to determine the photoluminescent quantum yield (PLQY) [11] of the upconverter or electrically determined EQE [3, 7] of an UC-PV device. The EQE is the ratio of photons incident at a given wavelength to electron-hole pairs collected across the junction. The PLQY is an optical measure of the UC material alone and is defined as,

$$\text{PLQY} = \frac{\text{No. of Photons Emitted}}{\text{No. of Photons Absorbed}} \quad (1)$$

where the integral of the photons emitted at shorter wavelengths is divided by the total number of excitation photons absorbed in relation to a non-luminescent reference. The

measurement of PLQY allows one to determine the upper limit of how effective a material is as a spectral converter in conjunction with a PV device. As the emission of UC photons has a quadratic dependence with excitation intensity (I_0), the PLQY follows a linear relation (see Eq. (2)).

$$\begin{aligned} \text{No. of Photons Emitted} &\propto I_0^2 \\ \text{PLQY} &\propto \frac{\text{No. of Photons Emitted}}{I_0} \propto I_0 \Rightarrow \log(\text{PLQY}) \propto 1 \times \log(I_0) \end{aligned} \quad (2)$$

However, there are many possible loss mechanisms when implemented within a real device; reflection at the interface of the cell, absorption within the host material and scattering, which applies to excitation and emission photons. The UC photons that reach the cell generate an electrical current dependant on the EQE of the device at that wavelength. The increase in the current of the device is proportional to the incident photon flux from the upconverter; therefore it is also proportional to the PLQY. Moreover, as the current is linear with PLQY, large solar concentrations are desirable to achieve better performance. Hence, in practice, UC-PV will likely be part of a concentrating photovoltaic (CPV) system. It is therefore essential to investigate methods that can achieve high PLQY at relatively low solar concentrations.

Recently, the focus has moved towards using broadband excitation to understand the efficiency of UC materials and devices under conditions closer to their application in solar energy. The first to suggest broadband excitation of UC was Balushev *et al.* [12], with a refined method being presented later [13]. However, these authors presented no measurements of PLQY for ultra-broad (40 nm bandwidth) excitation. Their experiments were performed on organic UC materials, which absorb and emit at 700 nm and 500 nm, respectively; a region where Si PV devices already perform very well. Therefore, these materials would not be used for the same application as Er^{3+} upconverters. More recent work on the EQE of an UC-PV device showed a considerable increase in EQE from 0.71% (at 1523 nm) to 1.07% using a xenon lamp for broadband excitation [14]. However, a detailed description of the illumination spectra was omitted and no extrapolation of PLQY was performed. Therefore, there exists a lack of basic understanding of UC through analysis of PLQY under a controlled broadband excitation spectrum in order to more fully evaluate the potential of UC for Si PV devices under concentrated sunlight.

2. Materials and method

In the present study, the PLQY of $\beta\text{-NaYF}_4$: 10% Er^{3+} in a fluorinated polymer was measured under broadband excitation with full width half maxima (FWHM) ranging from 12 to 80 nm. The phosphor powder $\beta\text{-NaYF}_4$: 10% Er^{3+} was prepared as described by Krämer *et al.* [15]. The powder was then embedded into a fluorinated polymer, perfluorocyclobutyl (PFCB, Tetramer Inc., USA), with a 55.6 w/w% and cured at 160°C for 18 hrs. The final sample was polished to a flat surface with dimensions of 1 mm in thickness and a diameter of 10 mm. The benefit of using PFCB is that fluorine replaces the C-H bonds that absorb the excitation light [16] and therefore an increased performance within an UC-PV device can be achieved. This is the first time that $\beta\text{-NaYF}_4$: Er^{3+} has been measured within PFCB.

The PLQY of the samples were measured using a calibrated spectrofluorometer (Edinburgh Instruments, FLS920) equipped with an integrating sphere (Jobin-Yvon) and a liquid nitrogen cooled NIR photon multiplier tube (PMT; Hamamatsu, R-5587). The PLQY was only measured for the transition $^4\text{I}_{11/2} \rightarrow ^4\text{I}_{15/2}$ (in the 980nm range) as this accounts for approximately 97% of UC emission [17]; thus, including higher photon emission in the calculation would increase PLQY only fractionally. The reference sample used was an undoped $\beta\text{-NaYF}_4$ powder cast in PFCB to represent the same scattering profile and to

remove any absorption/emission of the inorganic lattice and polymer matrix. The calibration uncertainty for this system is $\pm 3\%$ relative. Broadband excitation was achieved by adapting the spectrofluorometer for use with a 6 W supercontinuum (SC) laser and bandwidth selection from a high power acousto-optical tunable filter (AOTF-HP), both from Fianium (UK). The AOTF allows for 1 to 8 channels to simultaneously excite the sample; all with a given central wavelength, a FWHM of 12 nm, and an adjustable power defined by a variable radio frequency (RF) driver. As UC is non-linear with excitation power, the power flux was measured using a calibrated germanium (Ge) photodiode (Newport, 818-IR) and an IR imaging camera (Electrophysics MicronViewer 7290A), with beam diagnostic software to determine the area from the FWHM. The combined error of the calibration and the uncertainty associated with a digital display with respect to power flux is $\pm 4.4\%$.

Previous work in this field has only shown analysis in relation to the air-mass 1.5 global (AM1.5G) spectrum [7, 8, 14], which is the standard spectrum for characterizing PV devices under non-concentrated sunlight. However, terrestrial concentrator cell and module efficiencies **are** measured under the air-mass direct beam (AM1.5D, ASTM G-173-03) spectrum at an intensity of 900 W/m^2 and a cell temperature of 25°C . With respect to the intensity required for UC-PV, it is proposed that the AM1.5D spectrum should be the standard method of reporting. The broadband excitation used here requires an additional analysis and method of reporting, to clarify the difference between additional power under monochromatic excitation and increased power due to a larger bandwidth. The method used was to determine the FWHM of the excitation spectrum from the AOTF for bandwidths between 12 – 80 nm and compare this to the same bandwidth of the AM1.5D with the same central wavelength, λ_c . Additional measurement of the power flux for each bandwidth of excitation, allowed for the calculation of the solar concentration as described in Eq. (3):

$$\text{Solar Concentration} = \frac{\text{Excitation Power Flux}(\text{FWHM}, \lambda_c)}{\int_{\lambda_1}^{\lambda_2} \text{AM1.5d Power Flux}(\lambda) \cdot d\lambda} \quad (3)$$

where, $\lambda_1 = \lambda_c - (\text{FWHM} / 2)$ and $\lambda_2 = \lambda_c + (\text{FWHM} / 2)$ are the limits of integration. Therefore, all measurements are normalized to the solar spectrum, making increased bandwidth independent of increasing power and allowing one to analyze the performance in intuitive units. As these measurements were performed with a 1 nm resolution including the data for the AM1.5D spectrum an absolute uncertainty of $\pm 0.5 \text{ nm}$ in relation to the FWHM (associated with the power flux for a given excitation) under one sun (integrated power flux of 900 W m^{-2}) applies.

3. Results and discussion

Figure 2 shows the excitation spectra and describes how each channel is added to achieve greater bandwidths in an asymmetric/symmetric sequence, such that even channels increase bandwidth into the short-wavelength and odd channels into the long-wavelength end of the spectrum. The interplay of channel addition on peak photon counts makes it difficult to produce a flat top profile; however, the channel with the greatest variation in peak counts is within $\pm 5.5\%$ relative to its average. Furthermore, all the individual channel maximum peak counts are within 2.6% of the average of all the channels. This allows the effect of bandwidth to be determined independently of any change in intensity at a given wavelength. It can also be seen that the long and short wavelength FWHM points are well matched in relation to channel addition (Fig. 2). The AM1.5D spectrum in the wavelength range 1460 – 1600 nm has been plotted so as to allow one to compare the bandwidth used in excitation. Although

there is a close match in the spectra used; for bandwidths greater than 61nm there is less peak photon counts in the AM1.5D at wavelengths shorter than 1490nm.

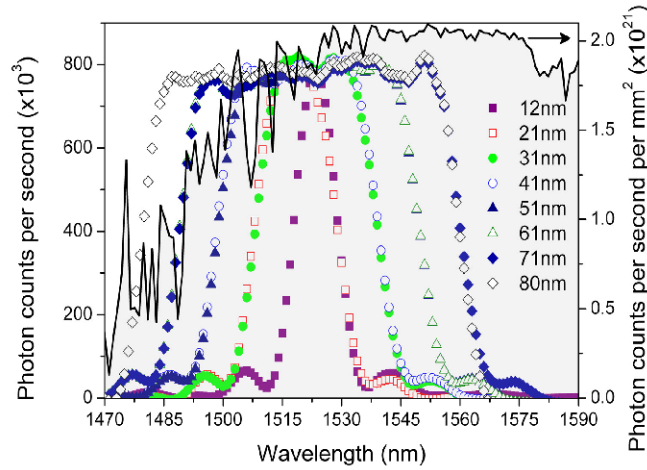


Fig. 2. Excitation scatter spectra used to achieve UC emission at 980 nm. The broadening of the spectrum due to additional channels from the AOTF can be seen as well as the asymmetric/symmetric sequence. The AM1.5D solar spectrum (grey shaded area) is also plotted against the secondary y-axis

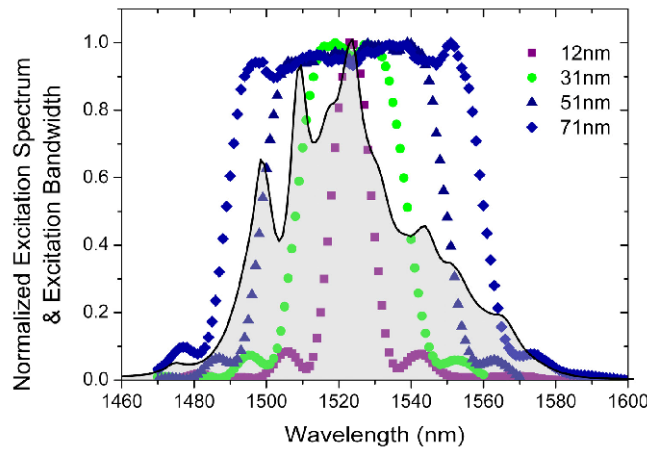


Fig. 3. Excitation wavelength dependence of achieving 980 nm UC emission with clear resonant peaks at 1523, 1509 and 1498 nm as shown by the grey shaded area. Increasing bandwidths encompass a larger portion of the excitation spectrum.

An excitation scan was performed to determine the most efficient wavelength range at which to excite the β -NaYF₄: 10% Er³⁺ to achieve emission at 980 nm (Fig. 3- grey shaded area). The excitation intensity for odd channels is shown to describe how the broadening of the spectrum encompasses a greater number of resonant peaks.

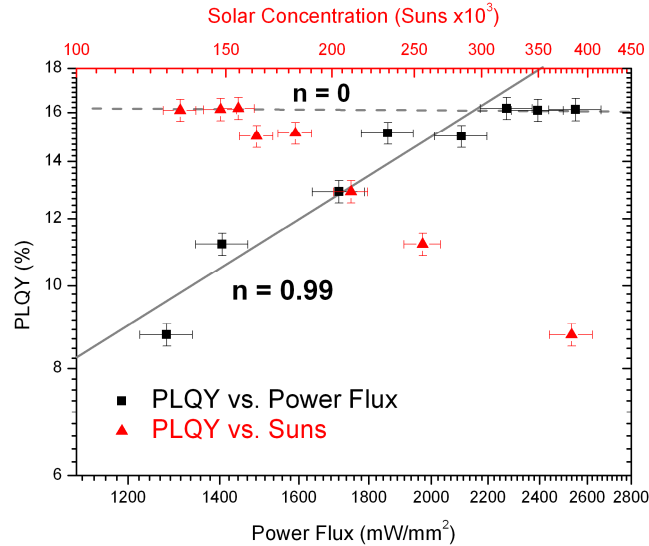


Fig. 4. The standard reporting method is shown (black squares) in comparison to the suggested “suns” method for broadband excitation (red triangles). These results show very high efficiencies, which improve with lower solar concentrations.

The results in Fig. 4 show the comparison of broadband excitation in relation to power flux and the newly proposed method of solar concentration to define the PLQY of the UC sample. In Fig. 4, it can be seen that the PLQY increases with higher power (black squares) due to the non-linear nature of the 2-photon UC process. The PLQY for the narrowest FWHM = 12 ± 0.5 nm is $8.7 \pm 0.3\%$. As the channel addition follows an asymmetric/symmetric step there is a large increase in PLQY followed by a smaller increase, respectively, until saturation at $16.2 \pm 0.5\%$ is reached. This can be explained by the excitation spectrum, which shows greater resonance and larger peaks on the shorter wavelength side of the maximum at 1523 nm (Fig. 3). Similarly, a lower resonance at longer wavelengths leads to a smaller increase in PLQY. Therefore, a broadening into the short-wavelength range encompasses a larger portion of the excitation spectrum and subsequent higher population of the $^4I_{13/2}$ level (GSA), a prerequisite for UC emission. It has been shown previously that ETU is the dominant mechanism for high concentrations of Er^{3+} (>2%) and within the NaYF_4 host under monochromatic excitation [4]. However, due to the broadband nature of the excitation spectrum, it is reasonable to assume that ESA has a higher contribution due to the presence of a wider range of resonant photons. Therefore, in comparison to monochromatic excitation, where the highest efficiencies are reported at the greatest resonant wavelength; the synergistic effect of exciting multiple resonant peaks associated with the individual transitions ($^4I_{15/2} \rightarrow ^4I_{13/2}$ and $^4I_{13/2} \rightarrow ^4I_{9/2}$) leads to an improved performance. Validation of this hypothesis requires careful analysis of photoluminescence decay measurements and will be investigated fully in a future work. Once the bandwidth increase surpasses these peaks (> 61 nm) there is a reduction in this effect, hence the PLQY saturates and only experimental error causes variation. The PLQY of 16.2% is the highest value reported in the literature for an UC material known to the authors. This value was measured at 61 ± 0.5 nm bandwidth with a central wavelength of 1519 nm and a power of 2270 ± 100 mW mm⁻². The reader should note that a PLQY of 16.2% represents the conversion of over 32% of the absorbed photons. The absorption of the sample was measured to be on average 20.8% in this region, which equates to an optical efficiency (a ratio of *emitted* photons to *incident* photons) of 3.4%. The previous highest efficiency was for an Er^{3+} doped ZBLAN glass investigated by Ivanova and Pellé [11] with a PLQY of 12.7%. The

result achieved in this work is also slightly higher to the PLQY of 16% which was measured for an organic upconverter [18] (with absorption at 670 nm this does not apply to Si devices). To make some reference to monochromatic excitation (as this is not possible with the AOTF) the same sample was measured using a tunable laser (HP Agilent, 8168F) with a power of $38 \pm 2 \text{ mW mm}^{-2}$ at the absorption peak of 1523nm. The attained efficiency was $1.1 \pm 0.1\%$ however, due to the limited power from the tunable laser this does not make for good comparison.

As the measurements saturate at a consistent value this validates the repeatability of these results for $\beta\text{-NaYF}_4$: 10% Er^{3+} through broadening of the excitation spectrum. Figure 4 is displayed in a double logarithmic plot, which allows the linear relation between PLQY and incident power to be observed (Eq. (2)). The gradient is calculated to be $n = 0.99$ for the data before saturation, which agrees with the theoretical value $n = 1$. Therefore, increasing bandwidth of excitation, while keeping the intensity per nm constant, follows the same relation to increasing power. For applications where a high PLQY is required one could use spectrally broader sources rather than increasing power at a given wavelength. Equivalently, the same PLQY can be archived with a factor of 1.9 less power with an increase in bandwidth of 5.1. The implication of this is that previous efficiencies for UC-PV devices could be achieved at lower powers or enhanced when illuminated by a broader spectrum.

When the PLQY is normalized to the power flux required, a value of $0.0007 \text{ cm}^2 \text{ W}^{-1}$ was calculated. This is a reporting method suggested by Auzel [10] to account for higher efficiencies at higher incident powers due to the non-linear behavior of UC. However, this analysis is limited at higher powers where the PLQY saturates and hence the normalized value decreases. This value is significantly lower than that reported by Fischer *et al.* [9], with a normalized efficiency of between $0.27\text{--}0.03 \text{ cm}^2 \text{ W}^{-1}$. Furthermore, it is also 1 order of magnitude lower than the result calculated by Richards *et al.* [8] of $0.07 \text{ cm}^2 \text{ W}^{-1}$ for an extrapolated efficiency of 16.7% although their measurements were performed with a higher Er^{3+} concentration ($\beta\text{-NaYF}_4$: 20% Er^{3+}).

The results in Fig. 4 are significant when presented in the new “suns” method, which accounts for a broadband excitation spectrum. When the same values of PLQY are plotted in relation to the solar concentration defined by Eq. (3) (corresponding to the equivalent power flux for a given bandwidth) an inverse relation is observed. As the bandwidth is increased so does the power due to the addition of further channels; however, an increase in bandwidth in relation to the solar spectrum also increases the incident power flux. For the bandwidths measured between 12 – 80 nm the excitation power flux used increases by a factor of 2 and equivalently a factor of 5, in relation to the AM1.5D spectrum. This means that although the power flux is increased, the actual solar concentration is reduced leading to an enhanced performance at a lower number of suns. Thus, the use of broadband excitation increases the available power without increasing the solar concentration. With comparison of the results achieved here, one can increase the PLQY by a factor of 1.9 with a reduction in solar concentration by a factor of 2.9 via utilization of a broader spectrum. This emphasizes the importance of the novel method for excitation and understanding the true potential of UC-PV devices.

Although the solar concentrations used in these measurements are beyond the diffraction limit achievable on Earth (45,000 suns limit [19]), they were performed on a sample that has neither been optimized in Er^{3+} concentration with the $\beta\text{-NaYF}_4$ host nor the loading factor of the phosphor within the polymer matrix. In addition, with the increased interest in the field of UC-PV and recent publications on the use of NIR quantum dots (QD) as spectral concentrators [20], it has been shown that performance of UC-PV devices can be improved. This can be achieved by absorbing the photons between the band edge of Si and the absorption range of Er^{3+} using QD's, which then emit in the range of the upconverter [21]. Moreover, the use of a PFCB host in the present study has the additional benefits when encapsulating NIR emitting QD's, with investigations indicating preservation of PLQY and

homogeneous dispersion [22]. The addition of these spectral concentrators would therefore make the efficiencies reported herein more readily achievable. Further investigation into the use of photonic structures for increasing the local electric-field surrounding the UC will also allow for greater intensities to be achieved under a lower factor of suns. A recent paper by Johnson *et al.* [23] modeled a 1-D photonic structure (commonly used as an anti reflection coating) to determine the enhancement of excitation light. Simulations showed that an enhancement factor between 2 and 18 could be achieved for 10 and 40 layer structures, respectively. However, as the enhancement factor increases the relative bandwidth decreases, which implies that optimization would be needed for broadband excitation. Moreover there is a large potential for the use of plasmonics for increasing the intensity of incident light through localized and propagating surface plasmons with possible enhancement factors of 450 times [24]. With these new advances in nano-materials and structures, in conjunction with analysis under broadband excitation, it is promising that the high PLQY reported here can be achieved under more realistic conditions and therefore dissemination of this technology.

4. Conclusions

To conclude, this is the first time that β -NaYF₄:Er³⁺ has been measured within PFCB and for any UC material under broadband excitation to determine the PLQY. The PLQY has been shown to increase from 8.7% to 16.2% by increasing the bandwidth from 12 nm to 61 nm, at which point the efficiency saturates for higher bandwidths. As this is the first time PLQY measurements have been reported for broadband excitation, a new method was developed to present the analysis in an intuitive way through solar concentration. The resulting PLQY of $16.2 \pm 0.5\%$ at $2270 \pm 100 \text{ mW mm}^{-2}$ ($0.0007 \text{ cm}^2 \text{ W}^{-1}$) or equivalently $155 \cdot 10^3 \pm 7 \cdot 10^3$ suns is the highest value reported in the literature. Although this is far beyond the solar concentration achievable on Earth, the measurements reported in the present study were performed on a sample without optimization of Er³⁺ concentration. Therefore future work will investigate the effect of Er³⁺ concentration; various loading factors of the phosphor into the host polymer matrix and additional lifetime analysis to understand better the UC mechanisms involved in broadband excitation. With an improved understanding on the limits of UC and in conjunction with enhancement from photonics and nano-materials, one can determine the true potential of UC-PV.

Acknowledgments

The authors would like to acknowledge the funding from the European Community's Seventh Framework Program (FP7/2007-2013) under grant agreement no. [246200] and Engineering and Physical Sciences Research Council (EPSRC) project "Luminescent Lanthanide Layers for Enhanced Photovoltaic Performance (LEAP)" (EP/I013245/1).